Saline groundwater evolution in Luanhe River Delta, China since Holocene: hydrochemical, isotopic and sedimentary evidence

Xianzhang Dang[a, b, c], Maosheng Gao[b, d], Zhang Wen[a], Guohua Hou[b, d], Hamza Jakada [e], Daniel Ayejoto[a], Qiming Sun[a, b,c]

[a]School of Environmental Studies, China University of Geosciences, 388 Lumo Rd, Wuhan, 430074, China

[b]Qingdao Institute of Marine Geology, CGS, Qingdao, 266237, China

[c]Chinese Academy of Geological Sciences, Beijing, 100037, China

[d]Laboratory for Marine Geology, Pilot National Laboratory for Marine Science and Technology, Qingdao, 266237, China

[e]Department of Civil Engineering, Baze University Abuja, Nigeria

Correspondence to: Maosheng Gao (gaomsh66@sohu.com), Zhang Wen (wenz@cug.edu.cn)

1   **Abstract**

2   Since the Quaternary Period, palaeo-seawater intrusions have been suggested to explain

3   the observed saline groundwater that extends far inland in coastal zones. The Luanhe

4   River Delta (northwest coast of Bohai Sea, China) is characterized by the distribution

5   of saline, brine, brackish and fresh groundwater, from coastline to inland, with a wide

6   range of total dissolved solids (TDS) between 0.38-125.9 g/L. Meanwhile, previous

7   studies have revealed that this area was significantly affected by Holocene marine

8   transgression. This study used hydrochemical, isotopic, and sedimentological methods

9   to investigate groundwater salinization processes in the Luanhe River Delta and its links

10 to the palaeo-environmental settings. The isotopic results (^{2}H, ^{18}O, ^{14}C) facilitate the

11 distinciton between old and new groundwater recharge. The hydro-chemical analysis

12 using PHREEQC indicates that the origin of salt in saline and brine groundwater is

13 from a marine source. The ^{18}O-Cl relationship diagram yields three end-member

14 groundwater mixing with two mixing scenarios suggested to explain the freshening and

15 salinization processes in the study area. When interpreted with data from palaeo-

16 environmental sediments, we found that groundwater salinization may have occurred

17 since the Holocene marine transgression. The brine is characterized by radiocarbon

18 activities of ~50 to 85 pMC and relatively depleted stable isotopes, which is associated

19 with seawater evaporation in the ancient lagoon during delta progradation and mixing

20 with deeper fresh groundwater which probably was recharged in cold late Pleistocene.

21 As for the brackish and fresh groundwater are characterized by river-like stable isotope

22 values where high radiocarbon activities (74.3 to 105.9 pMC) were formed after the

1   wash-out of salinized aquifer by surface water in the delta plain. This study presents an

2   approach for utilizing geochemical indicator analysis with paleogeographic

3   reconstruction to better assess groundwater evolutionary patterns in coastal aquifers.

Introduction

It is estimated that around 40% of the world's population lives in coastal areas (UN Atlas, 2010). Groundwater is an important freshwater resource for domestic consumption and agricultural activities in this region (Cary et al., 2015; Jayathunga et al., 2020). However, groundwater salinization poses a significant threat to everyday living and development activities (Tulipano, 2005; de Montety et al., 2008). In recent decades, groundwater salinization in coastal zones are widely concerned and studied. On the one hand, seawater intrusion due to groundwater pumping is a vital salinization process in the coastal aquifer (Reilly and Goodman, 1985; Werner, 2010, 2013; Han and Currell, 2018). On the other hand, groundwater salinization caused by the palaeo-seawater intrusion, in response to the Quaternary changes in global sea-level, has been reported in many coastal zones worldwide (Edmunds, 2001; Akouvi, 2008; Santucci et al., 2016, Larsen et al., 2017).

Coastal aquifers are linked to the ocean and continental hydrological cycle (Ferguson and Gleeson, 2012), both of which are influenced by natural and human-induced change (Jiao and Post, 2019). There is a steady-state seawater-freshwater interface under the natural state that extends inland from the coastal line (Costall et al., 2020). Since the Quaternary period, however, sea-level fluctuations on geological timescales have caused the interface to change, allowing seawater intrusion during transgression events and freshwater flushing during glacial low sea-level periods, which are evident in hydrochemical characteristics of groundwater in coastal aquifers(Kooi et al., 2000; Sanford, 2010; Aquilina et al., 2015; Lee et al., 2016). In addition, the hypersaline

groundwater found in coastal zones, particularly brine groundwater with a salinity of 2-4 times that of seawater, cannot be explained solely by using a seawater intrusion model (Sola et al., 2014, Han et al., 2020), and palaeoenvironment settings must be taken into consideration (Van Engelen et al., 2019). Some studies, for example, attribute the presence of brine in Mediterranean countries to the evaporation of seawater in the lagoon system during the Holocene transgression (Giambastiani et al., 2013, Vallejos et al., 2018).

The Bohai Sea of northern China was affected by Late Pleistocene transgressive-regressive cycles, which caused various salinity palaeo-saltwater intrusion along the coastal aquifers (Du et al., 2015; Li et al., 2017). Several studies have applied geochemical methods to elucidate the origin of saline groundwater and the salinization processes under anthropogenic influence, including induced mixing brine water from adjacent aquifers caused by groundwater overexploitation in Laizhou Bay (Han et al., 2011, 2014; Liu et al., 2017; Qi et al., 2019). However, the association between groundwater salinization (especially brine formation) and palaeoenvironmental implications are still not clear. Thus, this study applies a range of chemical, isotopic and sedimentary indicators to examine the Luanhe River Delta (situated along the northwestern coast of Bohai Sea) to elucidate the groundwater salinization processes in relation to recharge, salt source, mixing behavior and palaeogeographic evolution. The overall goal is to understand the groundwater evolutionary pattern influenced by transgression/regression events in geologic time. The findings will be significant to aquifer remediation activities in the region as well as other similar sedimentary

environments around the world.

2 Background of the study area

The study area is located in northeastern Hebei Province, China, on the west coast of Bohai (Fig. 1a). The study area consists of alluvial fan and coastal delta, bounded by Holocene maximum transgression line (Xue, 2016). The delta area can be further divided into two parts: old delta between the Douhe River and the Suhe River, the new delta between the Suhe River and the modern Luanhe River (He et al., 2020). The geomorphology of the study area is inclined to the south and southwest with a slope of about 0.04-2‰. The temperate monsoon climate affects the average annual temperature of 12.5°C and annual rainfall of 601 mm (1956-2010), with 80% of the annual rainfall occurring between July and September.

2.1 Hydrogeology

The thickness of Quaternary sediments in the study area is about 400-500 m. According to the lithology and hydrogeological characteristics, the Quaternary aquifers are made up of four distinct aquifers (Fig. 1b): The First Holocene aquifer (Q_4) is a phreatic or semi-confined aquifer with a bottom depth of 15-30 m and is primarily composed of fine sand and slit, involving fresh, brackish, saline and brine groundwater (Dang et al., 2020). The second Late Pleistocene aquifer (Q_3), the third Middle Pleistocene aquifer (Q_2), and the fourth Early Pleistocene aquifer (Q_1), with bottom depths of 120-170 m, 250-350 m, and 350-550 m, respectively. They have confined aquifers primarily made up of medium sand and gravel (Niu et al., 2019). The first aquifer is mainly recharged by meteoric precipitation and lateral infiltration of surface

water (Li et al., 2013). The groundwater from the first aquifer is widely extracted for

irrigation in the alluvial fan areas. The largest salt farm in north China, the Daqinghe

Salt Farm, uses shallow brine groundwater for salt production in the delta area, where

agricultural activities are small. Except for the area of alluvial fan, the circulation

between phreatic and confined aquifers is weak. The deep groundwater in second, third,

and fourth aquifers are mainly recharged by a surrounding mountain range and mainly

discharged by human pumping (Ma et al., 2014).
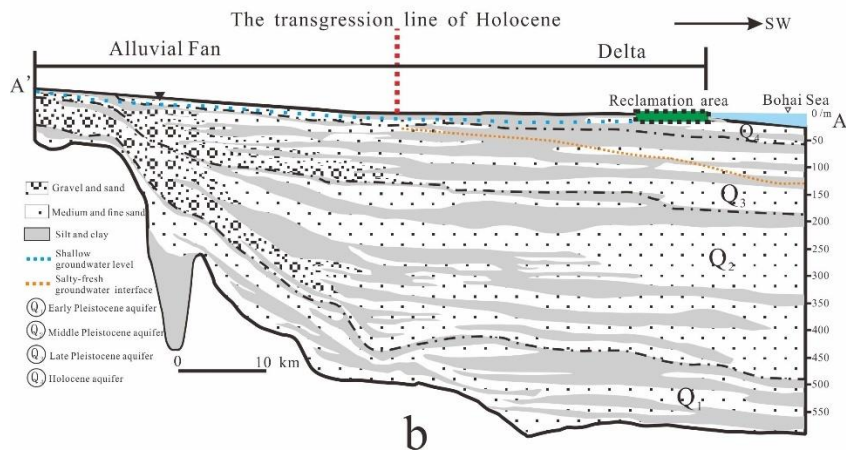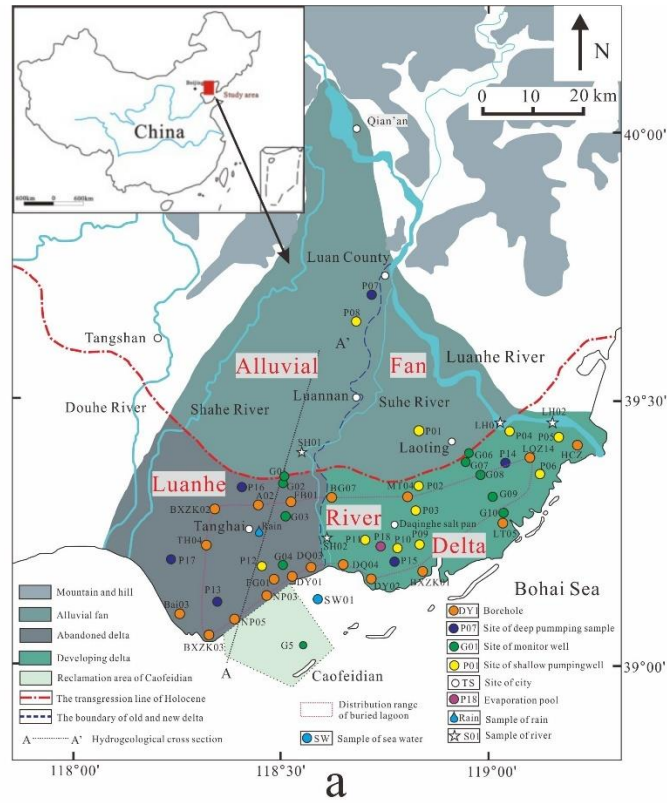
2   Fig. 1. (a) Location map of study area. Also shown are the sampling site and published cores in the

3   Luanhe River Delta. Cores LT05, HCZ, BXZK01, BXZK02 and BXZK03 were cited from He et

4   al. (2020); Cores NP05, NP03, DY01, DQ03, DQ04, DY02, MT04, BG07, FB01, A02 and TH04

5   were cited from Xu et al. (2020); Core LQZ04 was cited from Cheng et al. (2020); Core FG01 was

6   cited from Xu et al. (2011); Core Bai03 was cited from Li and Wang. (1983); Core HCZ was cited

7   from Peng et al. (1981). (b) Hydrogeological cross-section (A-A' in Fig. 1a) of study area,

8   modified by Ma et al., 2014.

2.2 Sedimentary evolution since the Late Pleistocene

Previous studies have shown that in the study region, the interface of salt-fresh groundwater gradually deepens from land (depth of ~ -5 m) to sea (depth of ~ -100 m), as shown in Fig. 1b, with salt groundwater primarily occurring in the first aquifer of the delta area (Li et al., 2013; Ma et al., 2014). According to stratigraphic transect along the present coastline (Fig. 2), the series stratigraphic architecture of the first aquifer consists of Late Pleistocene continental facies - Holocene marine facies – Holocene delta facies - modern continental facies or artificial fill, indicating that the sediments of the first aquifer had been deposited from lowstand continental accumulation to marine transgression and high stand progradation since the Late Pleistocene.

The seawater had not reached the modern coastline from the Last Glacial Maximum to the early Holocene (about 30-9 ka B.P.). The Luanhe alluvial fan was an activity in this period (He et al., 2020). Since about 9000 a B.P., the Holocene marine transgression approached the present coastline (Xu et al., 2020), and Holocene marine sediments developed under the sea-level rise from 9-7 ka B.P. The Holocene marine transgression had reached its maximum inland area 20 km from the modern coastline until about 7 ka B.P. (Gao et al., 1981; Peng et al., 1981; Xue, 2014, 2016) (Fig. 1 transgression line of Holocene), the accumulation of highstand prograding delta on top of Holocene marine strata, together with the artificial fill formed the modern coastal plain. In addition, lagoons are important components of the Luanhe River Delta (Feng and zhang, 1998). According to the records of lagoon facies in the published cores in this region, the approximate distribution range of buried lagoon is shown as a purple dashed line in Fig.

1   1a.
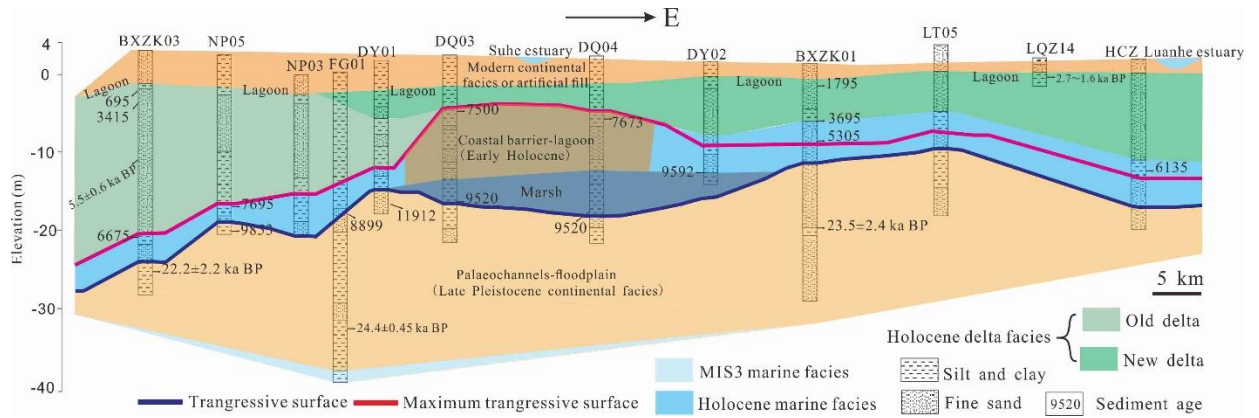
3   Fig.2 Stratigraphic transect along the present coastline of Luanhe River Delta, modified from He

4   et al.,2020.

5   3 Methods

6   In total, 45 water samples were collected from the Luanhe River Delta, including

7   38 groundwater samples, 5 surface water samples, 1 local rain water and 1 Bohai

8   seawater samples, during 4 sampling campaigns from October 2016 to June 2020.

9   Groundwater samples were divided into shallow groundwater samples and deep

10 groundwater samples, which were pumped from unconfined aquifer and confined

11 aquifer respectively. Surface water includes 2 Suhe River water samples and 2 Luanhe

12 River water samples. Due to artificial fill that has modified the coastal landscape, it was

13 difficult to locate the modern lagoon environment. However, during the investigation,

14 it was found that the Daqinghe salt farm in this area extracts seawater into the

15 evaporation pond. The mixture of seawater and meteoric water is subject to evaporation

16 to form concentrated saline water (CSW) in the pond, which is similar to the formation

17 of CSW in a coastal lagoon (Stumpp et al., 2014). Thus, 1CSW (P18 sample) in the

18 evaporation pond was collected.

Water types were classified according to Zhou (2013): freshwater (TDS < 1 g/L),

brackish water (TDS = 1 to 3 g/L), saline water (TDS = 3 to 50 g/L), and brine (TDS >

50 g/L). Groundwater sampling depths and pH values were measured on site using

CDT-divers. The concentrations of K^+, Na^+, Ca^{2+}, Mg^{2+}, and Br^- ion were measured

using inductively coupled plasma analysis (ICAP-7400), while SO_4^{2-} and Cl^- ions were

determined using ion chromatography (ICS-600). The HCO_3^- concentrations of samples

were measured using titration. The hydrochemical data are listed in Table S1(see

Supplement). The stable isotope concentrations (δ D, δ ^{18}O) of the water samples

(including G02-10, G06-10, G03-05, G04-40, G05-10, G05-46, G07-27, P07-20, P08-

30, P09-30, P10-30, P11-20, P12-40 P14-15, P07-100, P13-200, P14-300, P15-150,

P16-100, P17-200, P18, LH01, LH02, SH01, SH02, SW01, R1) were tested at the

Experimental & Testing Center of Marine Geology, Ministry of Natural Resource,

China, using High Temperature Pyrolysis-Isotope Ratio Mass Spectrometry. The values

of δ ^{18}O and δ D were calculated with respect to the Vienna Standard Mean Ocean Water

(VSMOW), and the uncertainty for δ D and δ ^{18}O are ±1.0‰ and ±0.2‰, respectively.

The radioisotope (AMS ^{14}C) of groundwater samples (P14-300, P15-150, and P16-100)

were measured at the Pilot National Laboratory for Marine Science and Technology.

Stable isotopes (δ D, δ ^{18}O, ^{13}C) and radioisotope of groundwater samples (G10-10,

G03-20, G04-15, G05-30, G06-15, G07-15, G08-15, G08-40, G09-15, G09-40, G10-

10, G10-30) were analyzed at the Beta Analytic TESTING LABORATORY, where the

δ ^{18}O and δ D values were also calculated with respect to VSMOW, and the uncertainty

for δ D and δ ^{18}O are listed in Table S1. The ^{14}C age of groundwater was calculated

1   using the following equation: $t = -8267 \cdot \ln\left(a_t{}^{14}C / q \cdot a_0{}^{14}C \right)$ (Clark and Fritz, 1997),

2   where t is radiocarbon ages in years Before Present (a B.P.); $a_t{}^{14}C$ is the measured ^{14}C

3   activity in % of modern carbon (pMC); $a_0{}^{14}C$ is the modern ^{14}C activity of soil derived;

4   q is a corrective factor, the corrective factor accounts for the dissolution of calcite,

5   which is assumed to be free of ^{14}C and, therefore, dilutes the initial ^{14}C activity of

6   aqueous DIC in recharged water. The results of ^{13}C, ^{14}C and the uncorrected residence

7   times are listed in Table S2.

8   **4 Results**

9   4.1 Hydrochemistry

10   Except for P13-200 (TDS=1.617 g/L, which is brackish water), all the deep

11   groundwater samples in the study region are freshwater. Deep groundwater

12   hydrochemical forms shift from $Ca-HCO_3$ to $Na-HCO_3$ as it moves from land to sea

13   (Fig. 3). For shallow aquifer, the horizontal interface of salt-fresh groundwater

14   corresponds better with the maximum Holocene transgression line (see Fig. 1a). The

15    $Ca-HCO_3$ type of shallow fresh groundwater is primarily distributed in the alluvial fan

16   region. The brackish and low TDS saline groundwater, which vary from $Ca-HCO_3$, $Na-$

17   HCO_3, and $Na-Cl$ types, are mainly contained in the upper aquifer (depth of 0-15 m) of

18   delta area, while the lower part (depth of 20–40 m) is $Na-Cl$ type of saline and brine

19   groundwater with high TDS. Moreover, for horizontal distribution of salinity, the

20   groundwater TDS tends to decrease from west to east, such as the TDS of saline and

21   brine groundwater TDS generally range from 16.57–125.97 g L^{-1} in old delta (western

22   delta), while 3.26–52.48 g L^{-1} in the new delta (eastern delta).
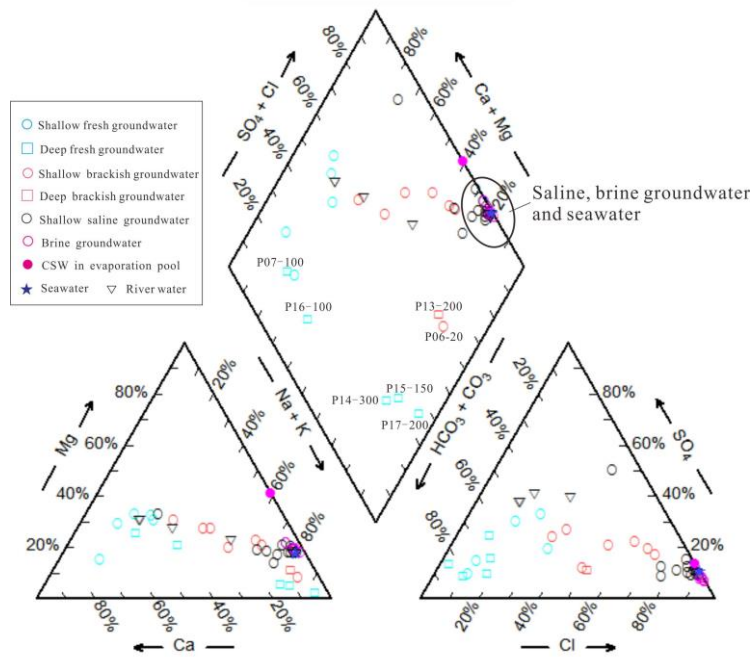
2   Fig. 3 Piper diagram of the various water samples.

3   4.2 ^{2}H, ^{18}O stable isotopes

4   Fig. 4 shows the relationship between deuterium and oxygen-18. The global meteoric

5   water line (GMWL, $\delta^2H=8\cdot\delta^{18}O+10$) is cited from Craig (1961), while the local

6   meteoric water line (LMWL, $\delta^2H=6.6\cdot\delta^{18}O+0.3$) is based on δ^2H and $\delta^{18}O$ isotope data

7   (1985-2003, mean monthly rainfall values) from the Tianjin station, about 100 km

8   southwest of the study area (IAEA/WMO, 2006). The deep groundwater samples

9   exhibit depleted values of stable isotopes, with values of δ^2H ranging from -75.52‰ to

10   -57.06‰ and $\delta^{18}O$ from -9.82‰ to -7.61‰. Shallow groundwater samples have heavier

11   hydrogen and oxygen isotope levels, ranging from -64.6 to -22.46% for δ^2H and -8.74

12   to -2.07% for $\delta^{18}O$. While the relatively small overall value of fresh and brackish

13   groundwater samples are similar to those of the river samples saline and brine

14   groundwater, were generally plotted below the LMWL or GMWL, which mean that the

1   water was subjected to evaporation prior to recharge into groundwater (Gibson et al.,

2   1993), or that multiple end-members mixing processes were involved (Han et al., 2011).
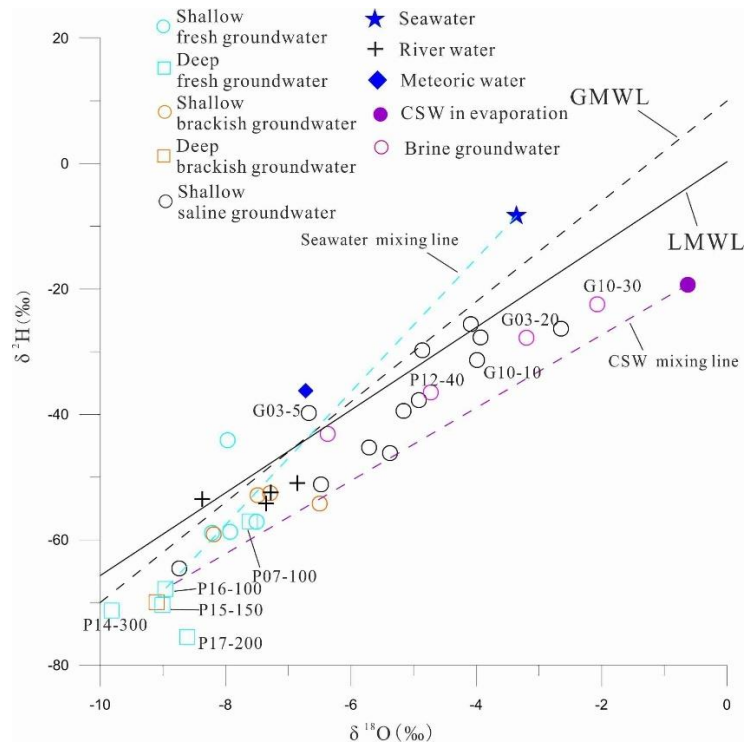
4   Fig. 4 Stable isotope compositions of different water samples. Seawater mixing line: mixing

5   between deep fresh groundwater and seawater; CSW mixing line: mixing between deep fresh

6   groundwater and CSW.

7   4.3 Groundwater residence times

8   The measured ^{14}C activities of groundwater samples range from 0.774 to 105.9 pMC

9   (Table S2). The properties of ^{14}C and sampling depth is shown in Fig. 5, which

10   elucidates the negative correlations, showing that variations of ^{14}C activities could be

11   attributed to radioactive decay aquifer. There are multiple processes that can impact the

12   [14]C properties including groundwater mixing and dispersion, long-term variation of

13   atmospheric ^{14}C and free ^{14}C dilution (e.g. carbonate dissolution) (Cartwright et al.,

14   2020). Due to the relative impact of these processes (which are not well established in

the study area), the uncertainty regarding the correction of radiocarbon ages to real

groundwater ages is very high. Consequently, we estimate groundwater age as a range

of the residence time. Uncorrected ages are considered the maximum age, while

corrected ages are the minimum age that are determined based on two hypothetical

models on carbonate dissolution that mainly affect the ^{14}C contents of water samples

(Lee et al., 2016).

Fig.5 shows activities of the ^{14}C in the shallow groundwater are within 30.6 to 105.9

pMC. These values indicate relatively modern recharge before atmospheric nuclear

testing period of the 1950s and 1960s. The radiocarbon activities in the deep fresh

groundwater are less than 12 pMC, which is consistent with the palaeo-water recharge.

This indicates that there are weak connection between shallow and deep aquifers.

Therefore, we assume that the shallow aquifer is an open system, while the deep aquifer

is a closed system. The δ^{13}C mixing and chemical mass balance (CMB) models are used

to estimate to corrective factor q, respectively (Clark and Fritz, 1997).

For δ^{13}C mixing model, $q = (\delta^{13}C_{DIC} - \delta^{13}C_{CARB})/(\delta^{13}C_{RECH} - \delta^{13}C_{CARB})$

(Pearson and Hanshaw, 1970), where $\delta^{13}C_{DIC}$ is the measured δ^{13}C of DIC in

groundwater; $\delta^{13}C_{CARB}$ is the δ^{13}C of DIC from dissolved soil mineral, using $\delta^{13}C_{CARB}$

= 1.5 ‰ (Chen et al., 2003); $\delta^{13}C_{RECH}$ is the δ^{13}C in water when it reaches the saturation

zone. In this study, we use a $\delta^{13}C_{RECH}$ of -15 ‰, which has been suggested as

appropriate for soils in northern China dominated by C_4 plants (Currell et al., 2010).

The model yielded some relatively low q values (0.59 of G06-15 and 0.65 of G08-15),

possibly since several unaccounted factors would contribute to variable $\delta^{13}C_{RECH}$ values,

1 e.g. local methanogenesis and pH or temperatures in the soil zones.

2 For CMB, $q = mDIC_{rech}/mDIC_{final}$, where $mDIC_{rech}$ is the DIC molar concentration

3 in the recharging water and $mDIC_{final}$ is the DIC molar concentration in the final

4 groundwater. $mDIC_{final}$ was   calculated   using:

5 $mDIC_{final} = mDIC_{rech} + [mCa + Mg - SO_4 + 0.5(Na + K - Cl)]$ (Fontes   and   Garnier,

6 1979). DIC_{rech} was mainly HCO_3 in the recharged water when pH values were between

7 6.4 and 10.3, and the carbonate equilibrium constant varies with temperature (Clark and

8 Fritz, 1997). $mDIC_{rech}$ was calculated from estimated pH and temperature condition for

9 the recharge environment, e.g., at pH = 6 and T = 15°C, the $mDIC_{rech}$ = 10 mmol/L

10 (Currell et al., 2010).

11 The corrected radiocarbon ages are shown in Table S2. The residence time of deep

12 groundwater ranged from 15959-39050 a B.P., which is significantly longer than that

13 of groundwater in the shallow aquifer (9510 a B.P. to modern). Moreover, most brackish

14 and fresh groundwater ages are modern, while brine has a longer residence period

15 (5590-1245 a B.P.) and a broader variety of saline groundwater samples.
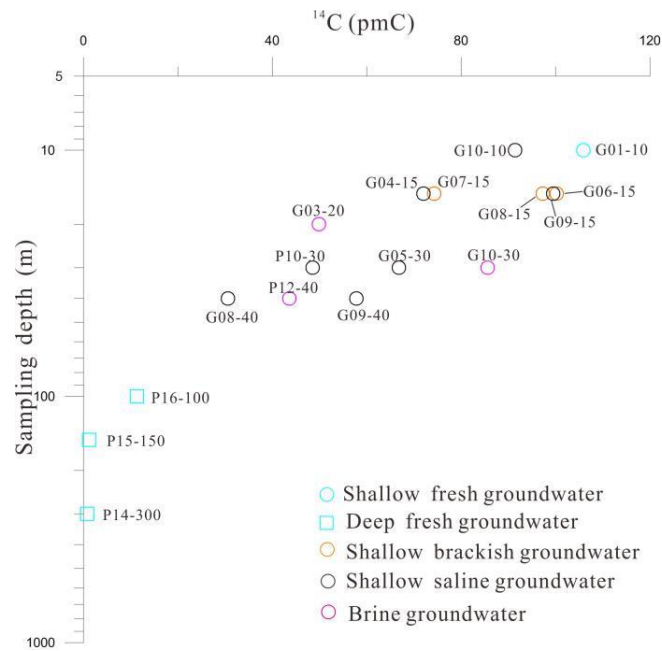
Fig. 5 ^{14}C activity with sampling depth in groundwater.

5 Discussion

5.1 Isotopic analysis for origin and recharge of groundwater

Deuterium and oxygen-18 are good tracers for groundwater origin and climatic conditions during recharge periods (Clark and Fritz, 1997). When combined with groundwater residence time, they could further identify modern and palaeo recharge (Han et al., 2014).

The depletion of ^{18}O and ^{2}H values in the deep fresh groundwater (Fig. 4) can be attributed to a cold climate (Kreuzer et al., 2009) and residence time of P15-150 and P14-300 samples (range from 33951 to 39050 a B.P) which may suggest that there was a recharge during the last glacial maximum. The stable isotopes of P16-100 are more heavier, reflecting the recharge history of warm climate in the previous deglaciation (Hendry and Wassenaar, 2000). The stable isotope values of river samples are similar to those of the shallow brackish and fresh groundwater compositions of the approximate

modern age, indicating lateral recharge of surface water locally. Meanwhile, in Fig. 4,

G03-5 is close to the rainfall sample, indicating that modern precipitation is a new

recharge source. The trend toward $\delta\,^2H$ and $\delta^{18}O$ enrichment in brine and saline

groundwater could be attributed to seawater infiltration during Holocene transgression

period, which has been confirmed by other study in Bohai Sea coast (Li et al., 2017, Du

et al., 2016). Additionally, due to the mixing of meteoric water and the subsequent non-

equilibrium fractionation of hydrogen isotope during evaporation (Clark and Fritz,

1997), the CSW sample is characterized by ^{18}O enrichment compared to seawater but

^2H depletion.

5.2 Hydrochemical analysis for sources of salinity

For distinguishing the sources of groundwater salinity, the PHREEQC code

(Parkhurst and Appelo, 2013) was used to measure and plot the theoretical seawater-

freshwater mixing line ("mixing line") and seawater evaporation line ("evaporation

line") using hydrogeochemical modeling. Using both simulation effects as references

to groundwater hydrochemical characteristics (Figs. 6and 7. For the Na-Cl (Fig. 6a),

Mg-Cl (Fig. 6b), and Br-Cl (Fig. 7a) diagrams, whose measured brackish, saline and

brine groundwater samples fit quite well to modeling mixing lines, and evaporation

lines follow linear trends from the least to the most saline. This would strongly

demonstrate that, the salt in these water samples is mainly of marine origin. The major

ions concentration in some samples (such as brine) is higher than those in the seawater,

suggesting the enriched ions are associated with evaporation processes rather than

seawater intrusion (Colombani et al, 2017).

Moreover, the samples deviate from the modeling lines (Fig. 6c and 6d), indicating that there may be other hydrogeochemical processes responsible for the modified ionic compositions (Giambastiani et al., 2013): (1) Ca^{2+} depletion of P18 and P12 samples are shown in Fig. 6d. This phenomenon is likely explained by gypsum ($CaSO_4$) precipitation. The evaporation line reveals that the Ca^{2+} composition of evaporating seawater follows a hooked trajectory (Fig. 6d). During evaporation to the point of gypsum saturation, residual CSW becomes progressively decreased Ca^{2+} concentration. (2) Ca^{2+} and SO_4^{2-} excess in most fresh and brackish samples (Fig. 6c and d) could be attributed to mineral dissolution along with stream water recharging (such as gypsum dissolution), highlighting some degree of dilution with continental runoff since Holocene regression. (3) Decomposition of organic matters abundant in marine or lagoon facies sediments can result in the release of bromide ions, thus making the Br/Cl ratios of saline groundwater samples higher than the mixing line (Fig. 7b).
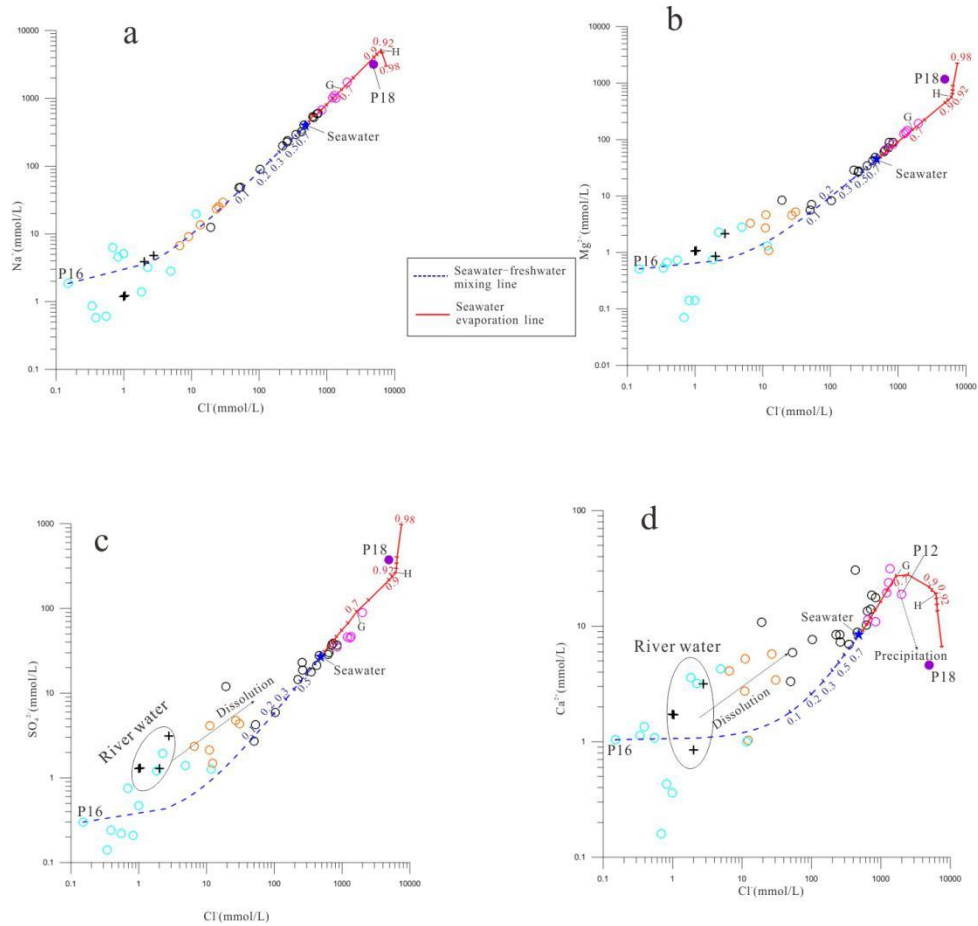
2   Fig. 6 Hydrochemical relationship between Cl and major ions of measured samples and simulated

3   results (seawater-freshwater mixing line: theoretical mixing between seawater and deep fresh

4   groundwater, and the blue numbers are mixing ratios of seawater; seawater evaporation line:

5   theoretical evaporation of Bohai seawater, and the red numbers are different evaporation rates) in

6   groundwater. G and H stand for point of precipitation of gypsum, halite respectively. The

7   "Dissolution" represents possible gypsum dissolution along with river water recharging. The

8   symbols of samples are same as Fig. 6.
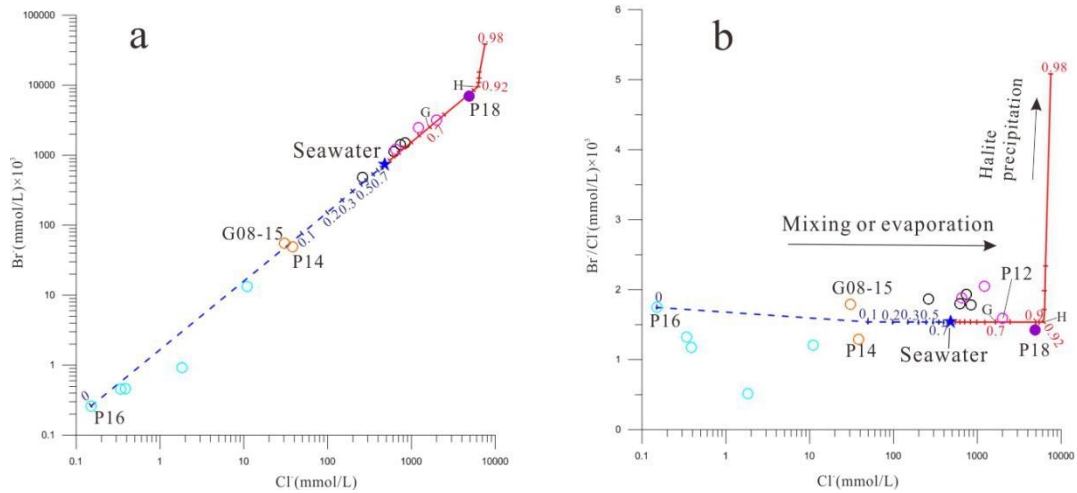
Fig. 7 Relationship between chloride and bromide content in water samples. Symbols are same as Fig. 6.

5.3 Mixing processes

Fig. 8 depicts the relationship between $\delta^{18}O$ and Cl⁻ in different water samples. There is a higher Cl- concentration and lighter δ18O values in brine samples than in seawater, meaning that simple two end-members mixing cannot adequately explain groundwater salinization. Stable isotopes of high TDS saline and brine samples fall between the seawater and CWS mixing lines, suggesting potential three end-member mixing processes (Douglas et al., 2000). Therefore, we considered SW01 (seawater) and P18 (most saline but with relatively depleted stable isotope) as two saline end-members. The P16-100, which is most likely recharged during the Last Deglaciation, was chosen to represent fresh end-members that could have been impacted by overlying seawater or CSW during Holocene transgression.–In Fig. 8, an inferred salinization zone was established that included almost all saline and brine groundwater samples, demonstrating the salinization processes in which fresh groundwater mixed with either seawater, CSW, or a mixture of both.

1   The fresh and brackish groundwater samples, on the other hand, have low Cl⁻

2   concentrations and lighter ^{18}O, deviating from the assumed salinization zone but

3   approaching the river samples in Fig. 8, implying a river water-groundwater mixing

4   trend. The LH02 (lighter $\delta^{18}O$) and SH02 (relatively heavier $\delta^{18}O$) were selected to

5   represent river water end-members range for different continental runoff in study area,

6   while the G09-15 (saline but with river-like stable isotope) was considered as a

7   groundwater end-member. There is a presumed freshening zone could form between

8   two river water-groundwater mixing lines, indicating occurrence of freshening

9   processes which would be in agreement with continental runoff dilution discussed in

10   section 5.2.
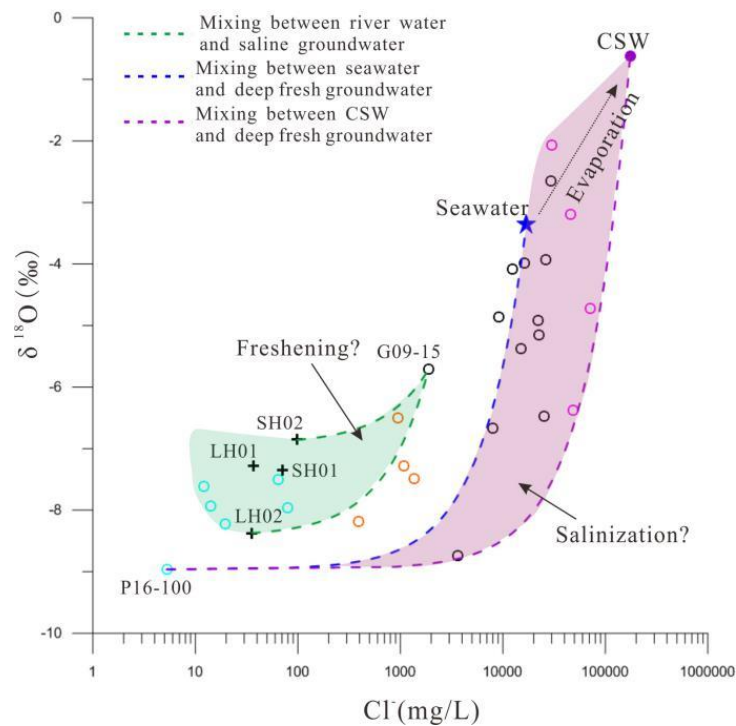
12   Fig. 8 Relationship between Cl and $\delta^{18}O$ of different water samples as means to various mixing

13   processes in the Luanhe River Delta. The symbols are same as Fig. 6. The green area is assumed

14   freshening zone, and the purple area is assumed salinization zone.

6 Interpretation of palaeo-environmental development

Based on analysis of a range of evidence related to Quaternary geographic evolution, it is possible to understand the change of hydrogeological conditions in the past (Van Engelen et al., 2018). The Pleistocene transgression events-related to Marine isotope stage (MIS) 3 and 5-have been observed to reach the study area by other authors once (Wang et al., 1981; Peng et al., 1981; Li et al., 1982; Li et al., 1983; Xu et al., 2018,), which would be resulted in groundwater salinization. Since the last deglaciation (about 15 ka B.P.), the palaeo-coast line has approximately 100 m depth below present sea level along the shelf edge (Li et al., 2014). Stronger river down-cutting and flushing in the study region would have been helped a large fresh recharge of groundwater. For example, P16-100 (fresh water) was sampled from a relatively deep position (100 m below surface) has an estimated groundwater age between 15959 to 17490 a B.P., which is likely to provide evidence that the salinization groundwater related to MIS 5 and/or 3 marine transgression could have been flushed out until the Latest Pleistocene. Accordingly, we believe that the observed saline groundwater in the Luanhe River Delta is probably related to the subsequent Holocene marine transgression. This research develops the evolutionary pattern of saline groundwater, as shown in Table 1 and Fig. Three phases are synthesized and reconstructed.

1   Table 1 Saline groundwater evolution processes in study area

Evolution stage	Groundwater evolution processes		Influencing factors			Major hydrogeochemical processes	Sediments
	Evolutionary pattern	Factors	Palaeoclimate	Geological setting	Others		
Phase 3 The development of new delta (3. 5ka B. P. to present)	Freshening	Wash-out of surface water	temperate, slightly semi-humid	Development of surface straem	irrigation return	Mixing and leaching	Holocene alluvial deposit or artificial fill Bottom sediments age about 1795—302 a B. P. (Xu et al., 2020 He et al., 2020)
	Deceleration of brine formation	Limitations of seawater evaporation		Diversion of channels and lagoon filled by diluvial deposit	artificial reclamation and offshore levees		Holocene lagoon facies Bottom sediments age about 5995—1600 a B. P. (Cheng et al., 2020 He et al., 2020)
Phase 2 The development of old delta (7 to 3. 5ka B. P.)	Brine formation	Sseawater evaporation and CSW infiltrating	temperate, slightly arid	Deceleration of sea-level rising, development of delta, and coastal lagoons have been active	Tides or storm	Mixing, leaching, evaporation, and mineral precipitation	Holocene delta facies Bottom sediments age about 6675—3695 a B. P. (He et al., 2020)
							Holocene marine facies Bottom sediments age about 8620—5595 a B. P. (Li et al., 1982)
Phase 1 Holocene transgression (12 to 7ka B. P.)	Groundwater salinization	Palaeo-seawater intrusion	temperate-warm, humid	Deglaciation of ice sheet, rapid rising of sea level, Holocene transgression		Mixing	Late Pleistocene continental facies (Xu et al., 2020 He et al., 2020)

Phase 1: Transgressive system tract-Holocene transgression stage (9-7 ka B.P.)

Global sea level was affected by deglaciation of the ice sheet (Fairbanks, 1989), causing sea level to rise rapidly during the deglaciation period (15.4-7 ka B.P.) (Li et al., 2014). It could be summarized that the Holocene transgression stage, which occurred between 9 and 7 ka B.P, resulted in the study area being inundated by seawater (Xu et al., 2015; Xue 2009, 2014) (Fig. 9a). On the one hand, there would have been a tendency for the denser seawater to infiltrate through the aeration zone (Santucci et al., 2016); on the other hand, sea-level rise would cause the seawater-freshwater interface to move landward (Ferguson and Gleeson, 2012), both of which contributed to palaeo-seawater intrusion. The G08-40 contains TDS of 27.173 g/L, which is more similar to that of SW01. Simultaneously, the residence time (9810-6884 a B.P.) indicates trapped palaeo-seawater at low-permeability aquitard sediments still exists and may be another critical salinity source for neighboring aquifers in the coastal zone (Post and Kooi, 2003; Lee et al., 2016).

The presence of palaeo-seawater intrusion during Quaternary has been recorded in other coastal regions worldwide (Groen et al., 2000; Bouchaou et al., 2009; Wang and

1   Jiao, 2012; Delsman et al., 2014;Tran et al., 2020; Han et al., 2020). For the works

2   described above, the salinity of groundwater after salinization could not exceed that of

3   seawater due to palaeo-seawater intrusion.

4   Other salinization processes that occurred during palaeo-environmental growth are

5   likely to be correlated with such brine groundwater.

6   *Phase 2: Highstand system tract-Old Luanhe River Delta development (7-3.5 ka B.P.)*

7   The good fit between the measured hydrochemistry and simulated evaporation lines

8   (Fig. 6 and 7) is an indicator that the brine samples were associated with the seawater

9   which was exposed to evaporation during geological history. Previous research has

10   revealed that lagoon was active during the progradation of the old Luanhe River Delta

11   between 7 and 3.5 ka B.P. (He et al., 2020; Xu et al., 2020). Meanwhile, the relatively

12   arid climate had been developed since 5500 a B.P., which may lead to increased

13   evaporation (Jin, 1984). The ancient lagoon would be an ideal location for evaporating

14   seawater that had been trapped due to storms or tides (Fig. 9b). As a result, concentrated

15   saline water (CSW) with salinity heavier than seawater would have created, and the

16   CSW would go through two processes: (1) infiltrating and descending to the lower part

17   of the aquifer due to its higher density, and combining with the salinized groundwater

18   from phase 1, resulting in a three end-members mixing scenario in the relationship

19   diagram (Fig. 8). (2) After reaching saturation during the later stages of evaporation,

20   mineral precipitation, such as gypsum, calcite, and halite, would occur, and this would

21   be subjected to redissolution by meteoric waters or seawater, resulting in high salinity

22   water that would then be subjected to the above process; The Br/Cl ratios in certain

fresh or brine groundwater samples deviate from the evaporation line (Fig. 7b), which

may be related to halite precipitation and redissolution. These two processes caused

groundwater salinity to rise even further, resulting in the formation of brine

groundwater with 3 times the TDS of seawater, such as G03-20 with a range of resident

time of 4323 to 5590 a B.P.

Phase 3: New Luanhe River Delta development (3.5 ka B.P. -present)

Since about 3500 a B.P., a nearly 90-degree diversion of the Luanhe River channel

in the study area resulted in new delta development (Wang et al., 2007; Xue, 2016).

There are some signs of a lagoon environment in the new Luanhe River Delta (Cheng

et al., 2020), and, as previously discussed, the brine groundwater sample G10-30 would

be attributed to evaporation in a lagoon setting (Fig. 9c). However, some factors are

likely to limit the CSW formation in the study area: (1) the relatively low evaporation

capacity due to semi-humid climate since about 2.5 ka B.P. (Jin, 1984), (2) the diluvial

deposit or artificial reclamation would have filled the coastal lowland such as lagoons,

and (3) offshore levees prevent the seawater from flooding inland during storms or tides.

Unlike the old Luanhe River Delta, these factors may also explain why the current

Luanhe River Delta does not have high TDS brine groundwater.

In addition, the brackish and low TDS saline groundwater with relatively modern age

(e.g. G09-15), and river-like stable isotopes (Fig. 4 and 8), are compelling evidence that

freshening processes have occurred in the delta plain. Since the semi-humid

palaeoclimate, some abandoned channels have developed into small rivers after the

diversion of the ancient Luanhe River (Gao, 1981), such as the Suhe River and Shahe

River. Firstly, the lateral recharge from the surface stream plays a role in washing out the salty groundwater. Secondly, due to the inefficiency of saline groundwater throughout human history, river irrigation has been commonly used for agricultural activities in the study region, freshening the upper saline aquifer (Fig. 9c). Some groundwater samples found above the seawater mixing line in the Ca-Cl and SO_4-Cl relationship diagrams (Fig. 6c, d) may be related to mineral dissolution during river water or irrigation recharge. However, saline groundwater can be washed out over time in coastal zones with low-permeable marine layers and a low hydraulic gradient (van Engelen et al., 2019; Han et al., 2020).

In summary, the evolution of saline groundwater in the study area results from palaeo-environment development such as sea-level change, palaeogeogrophy, and palaeoclimate, and is significantly affected by human activities. The coastal brine groundwater is a special product of geological evolution, which have been found in Bohai Sea coast such as Bohai Bay (Li et al., 2017) and Laizhou Bay (Han et al., 2014). The change in sea level over the Late Pleistocene would have favoured marine intrusion and similar sedimentary environment in Bohai coast, allowing this study infers the following conditions for its brine formation: (1) stable evaporative environments (e.g. lagoon), (2) suitable climatic conditions (e.g. arid), (3) seawater entering evaporative environments (e.g. storm or tide), and (4) long-term scale for salinity accumulation.
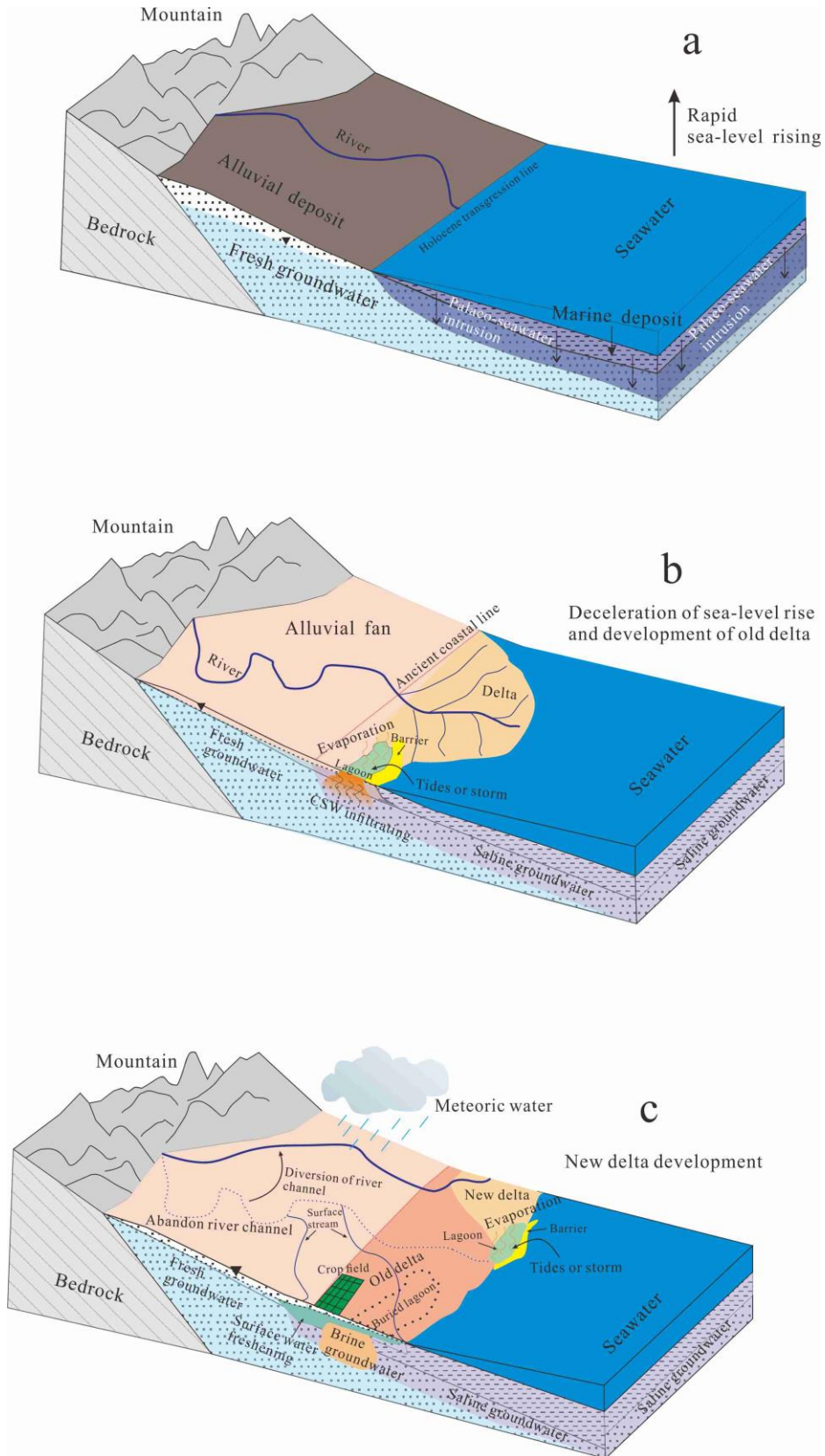
Fig. 9 Diagram of palaeoenvironmental development since Holocene and evolutionary pattern of

saline groundwater.

7 Conclusions

In this study, we used a range of isotopic-geochemical methods to analyze groundwater's recharge and salinity source in the Luanhe River Delta. The isotopic results (^{2}H, ^{18}O, ^{14}C) show that deep confined groundwater was recharged during the Late Pleistocene cold period, shallow saline and brine groundwater was recharged during the warm Holocene period, and shallow brackish and fresh groundwater was mainly recharged by surface water. The hydrogeochemical modeling (PHREEQC) results showe that seawater or evaporated seawater is the primary salty source in salinized groundwater. The variation in the ^{18}O-Cl relationship of multiple water samples further indicates multiple end-member mixing, which is useful assess the salinization and/or freshening processes in aquifers. Our study shows that multiple water types are particularly associated with complex geographic evolution in coastal areas. The variation in sea-levels (when it rises) causes lowland coastal areas to be inundated by seawater, which induces palaeo-seawater intrusion. The costal deltas developed after a significant drop in the sea levels. The concentration of saline water in the lagoon environment at the delta-front continuously provided salinity to the groundwater. Thus, brine groundwater was formed under the effects of evaporation, mixing, and dissolution. In contrast, the lateral recharge of surface water and irrigation return would cause slow wash-out of salinized groundwater in the delta plain.

Given that most coastal zones around the world experienced transgression/regression events in the Quaternary period, this work's findings will promote a better understanding of the origin of salinization in coastal aquifers. In addition, it is important

1   to recognize the potential leak of connate saline groundwater previously preserved in

2   adjunct aquifers that can occur due to the over-extraction of deep groundwater. To

3   effectively prevent pollution from saline groundwater movement, this study

4   recommends extensive characterization of groundwater interface dynamics, such as

5   fresh/saline, fresh/brine, and brine/seawater interfaces, and also maintain continuous

6   monitoring of water quality and levels across the aquifers

Authors contribution

Xianzhang Dang: Conceptualization, Formal analysis, Investigation, Writing-Original Draft, Data curation.

Maosheng Gao: Funding acquisition, Methodology, Supervision, Investigation, Writing-Review & Editing.

Zhang Wen: Supervision, Writing-Review & Editing.

Guohua Hou: Project administration, Investigation.

Hamza Jakada: Writing-Review & Editing.

Daniel Ayejoto: Writing-Review & Editing.

Qiming Sun: Investigation.

1 Acknowledgement

2   This study was financially supported by the National Natural Science Foundation

3 of China (U2106203, 41977173), National Geological Survey Project of China

4 Geology Survey (No. DD20211401) and China-ASEAN maritime cooperation fund

5 (Comparative Study of Geoenvironment and Geohazards in the Yangtze River Delta

6 and the Red River Delta). The authors would like to thank Sen Liu, Chenxin Feng, Chen

7 Sheng, Xueyong Huang and Haihai Zhuang, for their help and support in collecting

8 field data and conducting geological survey.

References

Akouvi, A., Dray, M., Violette S., et al.: The sedimentary coastal basin of Togo: example of a multilayered aquifer still influenced by a palaeo-seawater intrusion, HYDROGEOL. J., 16, 419-436, https://doi.org/10.1007/s10040-007-0246-1, 2008.

Aquilina, L., Vergnaud-Ayraud, V., Les Landes, A. A., et al.: Impact of climate changes during the last 5 million years on groundwater in basement aquifers, SCI. REP-UK, 5, 14132, https://doi.org/10.1038/srep14132, 2015.

Bouchaou, L., Michelot, J.L., Qurtobi, M., et al.: Origin and residence time of groundwater in the Tadla basin (Morocco) using multiple isotopic and geochemical tools, J. HYDROL., 379, 323-338, https://doi.org/10.1016/j.jhydrol.2009.10.019, 2009.

Cary, L., Petelet-Giraud E., Bertrand G., et al.: Origins and processes of groundwater salinization in the urban coastal aquifers of Recife (Pernambuco, Brazil): A multi-isotope approach, SCI. TOTAL. ENVIRON., 530-531, 411-429, https://doi.org/10.1016/j.scitotenv.2015.05.015, 2015.

Cartwright, I., Currell, M., Cendon, D., and Meredith, K.: A review of the use of radiocarbon to estimate groundwater residence times in semi-arid and arid areas, J. Hydrol., 580, 124247. https://doi.org/10.1016/j.jhydrol.2019.124247, 2020.

Chen, Z.Y., Qi, J.X., Xu, J.M.,et. al.: Paleoclimatic interpretation of the past 30 ka from isotopic studies of the deep confined aquifer of the North China Plain, APPL. GEOCHEM., 18, 997-1009, https://doi.org/10.1016/S0883-2927(02)00206-8,

2003.

Cheng, L.Y., Xu, Q.M., Guo, H., et al.: The Late Holocene Stratum and evolution in the Luanhe River Delta, Quaternary Sciences, 40(3), 751-763, https://doi.org/10.27355/d.cnki.gtjsy.2020.000012, 2020 (In Chinese with English abstract).

Clark, I.D., and Fritz, P.: Environmental Isotopes in Hydrogeology. Lewis Publishers, New York, 1997.

Colombani, N., Cuoco, E., Mastrocicco, M.: Origin and pattern of salinization in the Holocene aquifer of the southern Po Delta (NE Italy). J. GEOCHEM. EXPLOR., 175(2017): 130-137, https://doi.org/10.1016/j.gexplo.2017.01.011, 2017.

Costall A. R., Harris B. D., Teo B., et. al.: Groundwater Throughflow and Seawater intrusion in High Quality coastal Aquifers, SCI. REP-UK, 10: 9866, https://doi.org/10.1038/s41598-020-66516-6, 2020.

Craig, H.: Standard for reporting concentration of deuterium and oxygen-18 in natural water, SCIENCE, 133, 1833-1834, https://doi.org/10.1126/science.133.3467.1833, 1961.

Currell, M.J., Cartwright, I., Bradley, D.C., and Han, D.M.: Recharge history and controls on groundwater quality in the Yuncheng Basin, north China, J. HYDROL., 385, 216-229., https://doi.org/10.1016/j.jhydrol.2010.02.022, 2010.

Dang, X.Z., Gao, M.S., Wen, Z., et al.: Evolutionary process of saline groundwater influenced by palaeo-seawater trapped in coastal deltas: A case study in Luanhe River Delta, China, ESTUAR. COAST. SHELF. S., 244, 106894,

https://doi.org/10.1016/j.ecss.2020.106894, 2020.

de Montety, V., Radakovitch, O., Vallet-Coulomb, C., et al.: Origin of groundwater salinity and hydrogeochemical processes in a confined coastal aquifer: case of the Rhone delta (Southern France), APPL. GEOCHEM., 23(8), 2337-2349, https://doi.org/10.1016/j.apgeochem.2008.03.011, 2008.

Delsman, J. R., Huang, K. R. M., Vos, P. C., et., al.: Paleo-modeling of coastal saltwater intrusion during the Holocene: an application to the Netherlands, HYDROL. EARTH. SYST. SCI., 18(10), 3891-3905, https://doi.org/10.5194/hess-18-3891-2014,2014.

Douglas, M., Clark, I.D., Raven, K., et al.: Groundwater mixing dynamics at a Canadian Shield mine, J. HYDROL., 235, 88-103, https://doi.org/10.1016/S0022-1694(00)00265-1, 2000.

Du, Y., Ma, T., Chen, L., et al.: Genesis of salinized groundwater in Quaternary aquifer system of coastal plain, Laizhou Bay, China: Geochemical evidences, especially from bromine stable isotope, APPL. GEOCHEM., 2015, 59:155-165, https://doi.org/10.1016/j.apgeochem.2015.04.017, 2015.

Du, Y., Ma, T., Chen L., et al.: Chlorine isotopic constraint on contrastive genesis of representative coastal and inland shallow brine in China, J. GEOCHEM. EXPLOR., 170 (2016): 21-29, https://doi.org/10.1016/j.gexplo.2016.07.024, 2016.

Edmunds, W. M.: Palaeowaters in European coastal aquifers-the goals and main conclusions of the PALAEAUX project, Geological Society London Special Publications, 189, 1-16, https://doi.org/10.1144/GSL.SP.2001.189.01.02, 2001.

Fairbanks, R.G.: A 17,000-year glacio-eustatic sea level record: influence of glacial melting rates on the Younger Dryas event and deep ocean circulation, NATURE, 342, 637-647, https://doi.org/10.1038/342637a0, 1989.

Feng, J. and Zhang, W.: The evolution of the modern Luanhe River delta, north China, GEOMORPHOLOGY, 25 (3), 269-278, https://doi.org/10.1016/S0169-555X(98)00066-X, 1998.

Ferguson, G. and Gleeson, T.: Vulnerability of coastal aquifers to groundwater use and climate change, NAT. CLIM. CHANGE., 2, 342-345, https://doi.org/10.1038/nclimate1413, 2012.

Fontes, J.C., and Garnier, J.M.: Determination of the initial ^{14}C activity of the total dissolved carbon: a review of the existing models and a new approach. WATER. RESOUR. RES., 15 (2), 399–413, https://doi.org/10.1029/wr015i002p00399, 1979.

Gao, S.M.: Facies and sedimentary model of the Luan River delta. Acta Geographica Sinica, 48 (3), 303-314, 1981 (in Chinese with English abstract).

Giambastiani, B.M.S., Colombani, N., Mastrocicco, M. and Fidelibus, M.D.: Characterization of the lowland coastal aquifer of Comacchio (Ferrara, Italy): Hydrology, hydrochemistry and evolution of the system, J. HYDROL., 501: 35-44, https://doi.org/10.1016/j.jhydrol.2013.07.037, 2013.

Gibson, J.J., Edwards, T.W., Bursey, G.G., and Prowse, T.D.: Estimating evaporation using stable isotopes: quantitative results and sensitivity analysis for two catchments in Northern Canada, Nordic Hydrology. 24, 79-94,

https://doi.org/10.2166/nh.1993.0015, 1993.

Groen, J., Velstra, J., Meesters, A.: Salinization processes in paleowaters in coastal sediments of Suriname: evidence from $\delta^{37}Cl$ analysis and diffusion modelling, J. HYDROL., 234, 1-20, https://doi.org/10.1016/S0022-1694(00)00235-3, 2000.

Han, D.M., Kohfahl, C., Song, X.F., et al. : Geochemical and isotopic evidence for Palaeo-Seawater intrusion into the south coast aquifer of Laizhou Bay, China, APPL. GEOCHEM. 26 (5), 863-883, https://doi.org/10.1016/j.apgeochem.2011.02.007, 2011.

Han, D. M., Song, X. F., Currell, M. J., et al.: Chemical and isotopic constraints on the evolution of groundwater salinization in the coastal plain aquifer of Laizhou Bay,China, J. HYDROL., 508, 12–27, https://doi.org/10.1016/j.jhydrol.2013.10.040, 2014.

Han, D.M., and Currell, M.J.: Delineating multiple salinization processes in a coastal plain aquifer, northern China: hydrochemical and isotopic evidence, HYDROL. EARTH. SYST. SCI., 22, 3473-3491, https://doi.org/10.5194/hess-22-3473-2018, 2018.

Han, D.M., Cao G.L., Currell, M.J., et al.: Groundwater salinization and flushing during glacial-interglacial cycles: insights from aquitard porewater tracer profiles in the North China Plain, China, WATER. RESOUR. RES., 56 (11), https://doi.org/10.1029/2020WR027879, 2020.

He L., Amorosi A., Ye S.Y., et al.: River avulsions and sedimentary evolution of the Luanhe fan-delta system (North China) since the late Pleistocene, MAR. GEOL.,

425,106194, https://doi.org/10.1016/j.margeo.2020.106194, 2020.

Hendry, M.J. and Wassenaar, L.I.: Controls on the distribution of major ions in pore waters of thick surficial aquitard, WATER. RESOUR. RES., 36 (2), 503-513, https://doi.org/10.1029/1999WR900310, 2000.

IAEA/WMO: Global Network of Isotopes in Precipitation, The GNIP Database, Vienna, available at: http://www-naweb.iaea.org/napc/ih/IHS_resources_gnip. html (last access: 18 November 2013), 2006.

Jayathunga K., Diyabalanage S., Frank A.H., et al.: Influences of seawater intrusion and anthropogenic activities on shallow coastal aquifers in Sri Lanka: evidence from hydrogeochemical and stable isotope data, ENVIRON. SCI. POLLUT. R., 2020, 27(18), https://doi.org/10.1007/s11356-020-08759-4, 2020.

Jiao, J.J. and Post, V.: Coastal Hydrology. Cambridge University Press, New York, 2019.

Jin, X.F.: The spore-pollen assemblages and the stratigraphy and palaeogeography in western Bohai Sea since late Pleistocene, Marine Science Bullition 3, 16-24, 1984 (in Chinese with English abstract).

Kooi, H., Groen, J., and Leijnse, A.: Modes of seawater intrusion during transgressions, WATER. RESOUR. RES., 36, 3581–3589, https://doi.org/10.1029/2000wr900243, 2000.

Kreuzer, A.M., Rohden, C.V., Friedrich, R., et al.: A record of temperature and monsoon intensity over the past 40 kyr from groundwater in the North China Plain, CHEM. GEOL., 259, 168-180, https://doi.org/10.1016/j.chemgeo.2008.11.001, 2009.

Larsen, F., Tran, L. V., Van Hoang, H., et. al.: Groundwater salinity influenced by

Holocene seawater trapped in incised valleys in the Red River delta. NAT. GEOSCI., 10, 376-381, https://doi.org/10.1038/ngeo2938, 2017.

Lee, S., Currell, M., and Cendon, D. I.: Marine water from mid-Holocene sea level highstand trapped in a coastal aquifer: Evidence from groundwater isotopes, and environmental significance, SCI. TOTAL. ENVIRON., 544, 995-1007, https://doi.org/10.1016/j.scitotenv.2015.12.014,2016.

Li, G.X., Li, P., Liu, Y., et al.: Sedimentary system response to the global sea level change in the East China Seas since the last glacial maximum, EARTH-SCI. REV., 139 (2014), 390-405, https://doi.org/10.1016/j.earscirev.2014.09.007, 2014.

Li, H.M. and Wang, J.D.: Palaeomagnetic study on drill core from northern Bohai coastal plain. Geochimica, 2, 196-204,1983 (in Chinese with English abstract).

Li, J., Liang, X., Jin, M. G., et al.: Geochemical signature of aquitard pore water and its paleo-environment implications in Caofeidian Harbor, China, GEOCHEM. J., 47, 37-50, https://doi.org/10.2343/geochemj.2.0238, 2013.

Li, Y.F., Gao, S.M. and An, F.T.: A preliminary study of the Quaternary marine strata and its paleogeographic significance in the Luanhe delta region, Oceanologia et Limnologia Sinica, 13 (5), 433-439, 1982 (in Chinese with English abstract).

Liu, S., Tang, Z., Gao, M. et al.: Evolutionary process of saline-water intrusion in Holocene and Late Pleistocene groundwater in southern Laizhou Bay, SCI. TOTAL. ENVIRON., 607-608, 586-599, https://doi.org/10.1016/j.scitotenv.2017.06.262, 2017.

Ma, F. S., Wei, A. H., Deng, Q. H., et al.: Hydrochemical Characteristics and the Suitability of Groundwater in the Coastal Region of Tangshan, China, J. EARTH

SCI-CHINA, 26 (6), 1067-1075, https://doi.org/10.1007/s12583-014-0492-9, 2014.

Niu, Z.X., Jiang X.W. and Hu, Y.Z.: Characteristics and causes of hydrochemical evolution of deep groundwater in the Luanhe delta, Hydrogeology and Engineering Geology, 46 (01), 27-34, 2019 (in Chinese with English abstract).

Parkhurst, D.L., Appelo, C.A.J.: Description of input and examples for PHREEQC version 3-a computer program for speciation, batch-reaction, one-dimensional transport, and inverse geochemical calculations, U.S. Geological Survey Techniques and Methods, book 6, chap. A43, 497 pp., available only at http://pubs.usgs.gov/tm/06/a43/, 2013.

Peng, G., Jiao, W.Q., Li, D.M., and Li, G.Y.: Division and correlation of the late Quaternary stratigraphy and discussion on the recent tectonic movement in the region of the Luanhe River Delta, Seismoloqy and Geology, 3, 31-36, 1981 (in Chinese with English abstract).

Pearson, F.J. and Hanshaw, B.B.: Sources of dissolved carbonate species ingroundwater and their effects on carbon-14 dating. In: IAEA (Ed.), Isotope Hydrology, IAEA, Vienna, 1970.

Post, V. E. and Kooi, H.: Rates of salinization by free convection in high-permeability sediments: insight from numerical modeling and application to Dutch coastal area, HYDROGEOL. J., 11, 549-559, https://doi.org/10.1007/s10040-003-0271-7, 2003.

Qi, H., Ma, C., He, Z., et al.: Lithium and its isotopes as tracers of groundwater

salinization: A study in the southern coastal plain of Laizhou Bay, China, SCI. TOTAL. ENVIRON., 650:878-890, https://doi.org/10.1016/j.scitotenv.2018.09.122, 2019.

Reilly, T. E. and Goodman, A. S.: Quantitative analysis of saltwater-freshwater relationships in groundwater systems-a historical perspective, J. HYDROL., 80, 125-160, https://doi.org/10.1016/0022-1694(85)90078-2, 1985.

Sanford, W.E.: Groundwater hydrology: Coastal flow, NAT. GEOSCI., 3, 671-672, https://doi.org/10.1038/ngeo958, 2010.

Santucci, L., Carol, E., Kruse E.: Identification of palaeo-seawater intrusion in groundwater using minor ions in a semi-confined aquifer of the Río de la Plata littoral (Argentina), SCI. TOTAL. ENVIRON., 566-567, 1640-1648, https://doi.org/10.1016/j.scitotenv.2016.06.066, 2016.

Sola F., Vallejos A., Daniele L., Pulido-Bosch A.: Identification of a Holocene aquifer-lagoon system using hydrogeochemical data, QUATERNARY RES., 82,121-131, https://doi.org/10.1016/j.yqres.2014.04.012, 2014.

Stumpp, C., Ekdal, A., Gonenc, I.E. and Maloszewski, P.: Hydrological dynamics of water sources in a Mediterranean lagoon, HYDROL. EARTH. SYST. SCI., 18, 4825-4837, https://doi.org/10.5194/hess-18-4825-2014, 2014.

Tulipano, L., Fidelibus, M.D., Panagopoulos, A.: COST ACTION 621 Final Report, Groundwater Management of Coastal Karstic Aquifers, Office for the Official Publications of European Communitied, Luxembourg, Vol. Ⅱ,366pp., ISBN 92-894-0015-1,2005.

1   Tran, D.A., Tsujimura M., Vo L.P., et al: Hydrogeochemical characteristics of a multi-

2   layered coastal aquifer system in the Mekong Delta, Vietnam, ENVIRON.

3   GEOCHEM. HLTH., 42, 661-680, https://doi.org/10.1007/s10653-019-00400-9,

4   2020.

5   UN Atlas: 44 Percent of us Live in Coastal Areas, available at:

6   http://coastalchallenges.com/2010/01/31/un-atlas-60-of-us-live-in-the-coastal-

7   areas, 2010.

8   Vallejos A., Sola F., Yechieli Y., et. al.: Influence of the paleogeographic evolution on

9   the groundwater salinity in a coastal aquifer. Cabo de Gata aquifer, SE Spain. J.

10   HYDROL., 557,55-66, https://doi.org/10.1016/j.jhydrol.2017.12.027, 2018.

11   van Engelen J., Oude E., Gualbert H.P., et al.: On the origins of hypersaline

12   groundwater in the Nile Delta aquifer, J. HYDROL., 560, 301-317,

13   https://doi.org/10.1016/j.jhydrol.2018.03.029, 2018.

14   van Engelen J., Verkaik J., King J., Nofal E.R., et al.: A three-dimensional

15   palaeohydrogeological reconstruction of the groundwater salinity distribution in

16   the Nile Delta Aquifer, HYDROL. EARTH. SYST. SCI., 23, 5175-5198,

17   https://doi.org/10.5194/hess-23-5175-2019, 2019.

18   Wang, P.X., Min, Q.B., Bian, Y.H. et al.: Strata of Quaternary transgressions in east

19   China: A preliminary study. Acta Geologica Sinica, 1981 (01), 1-13, 1981 (in

20   Chinese with English abstract).

21   Wang, Y. and Jiao, J.J.: Origin of groundwater salinity and hydrogeochemical processes

22   in the confined Quaternary aquifer of the Pearl River Delta, China, J. HYDROL.,

438-439, 112-124, https://doi.org/10.1016/j.jhydrol.2012.03.008, 2012.

Wang, Y., Fu, G., Zhang, Y.: River-sea interactive sedimentation and plain morphological evolution, Quaternary Science, 27, 674-689, https://doi.org/10.3321/j.issn:1001-7410.2007.05.009, 2007(in Chinese with English abstract).

Werner, A. D.: A review of seawater intrusion and its managementin Australia, HYDROGEOL. J., 18, 281-285, https://doi.org/10.1007/s10040-009-0465-8, 2010.

Werner, A. D., Bakker, M., Post, V. E. A., et al.: Seawater intrusion processes, investigation and management: Recent advances and future challenges, ADV. WATER RESOUR., 51, 3-26, https://doi.org/10.1016/j.advwatres.2012.03.004, 2013.

Xu, Q.M., Yuan, G.B., Zhang, J.Q., et al.: Stratigraphic division of the Late Quaternary strata along the coast of Bohai bay and its geology significance, Acta Geologica Sinica, 85 (8), 1352-1367, 2011 (in Chinese with English abstract).

Xu, Q.M., Yang, J.L., Yuan, G.B.,et. al.: Stratigraphic sequence and episodes of the ancient Huanghe Delta along the southwestern Bohai Bay since the LGM, MAR. GEOL., 367, 69-82, https://doi.org/10.1016/j.margeo.2015.05.008, 2015.

Xu, Q.M., Yang, J.L., Hu, Y.Z., et. al.: Magnetostratigraphy of two deep boreholes in the southwestern BohaiBay: its tectonic implications and constraints on ages of volcanic layers, QUAT. GEOCHRONOL., 43, 102-114, https://doi.org/10.1016/j.quageo.2017.08.006, 2018.

Xu, Q.M., Meng, L.S., Yuan, G.B., et al.: Transgressive wave-and tide-dominated barrier-lagoon system and sea-level rise since 8.2 ka recorded in sediments in northern Bohai Bay, China, GEOMORPHOLOGY, 352, 106978, https://doi.org/10.1016/j.geomorph.2019.106978, 2020.

Xue, C.T.: Historical changes of coastlines on west and south coasts of Bohai Sea since 7000 a B.P.. Scientia Geographic Sinica, 29, 217-222, https://doi.org/10.3969/j.issn.1000-0690.2009.02.012, 2009 (in Chinese with English abstract).

Xue, C.T.: Missing evidence for stepwise postglacial sea level rise and an approach to more precise determination of former sea levels on East China Sea Shelf. MAR. GEOL., 348, 52-62, https://doi.org/10.1016/j.margeo.2013.12.004, 2014.

Xue, C.T.: Extents, type and evolution of Luanhe River fan-delta system, China. Marine Geology & Quaternary Geology, 36 (06), 13-22, 2016 (in Chinese with English abstract).

Zhou, X.: Basic characteristics and resource classification of subsurface brines in deep-seated aquifers. Hydrogeology & Engineering Geology, 40 (5), 4-10, 2013 (in Chinese with English abstract).